

Supporting Information

Manganese-nickel bimetallic oxide electrocatalyzing redox reactions of lithium polysulfide in lithium-sulfur batteries

Yu Si,^{ab} Jizong Zhang,^{ab} Qiumi Huang,^{ab} Jianghai Wei,^{ab} Chengyang Wang,^{ab} Kemeng Ji^{ab} and Mingming Chen^{*ab}

- a. *Key Laboratory for Green Chemical Technology of MOE, School of Chemical engineering and Technology, Tianjin University, Tianjin 300072, P. R. China. Email: chmm@tju.edu.cn.*
- b. *Collaborative Innovation Center of Chemical Science and Engineering (Tianjin), Tianjin University, Tianjin 300072, P. R. China.*

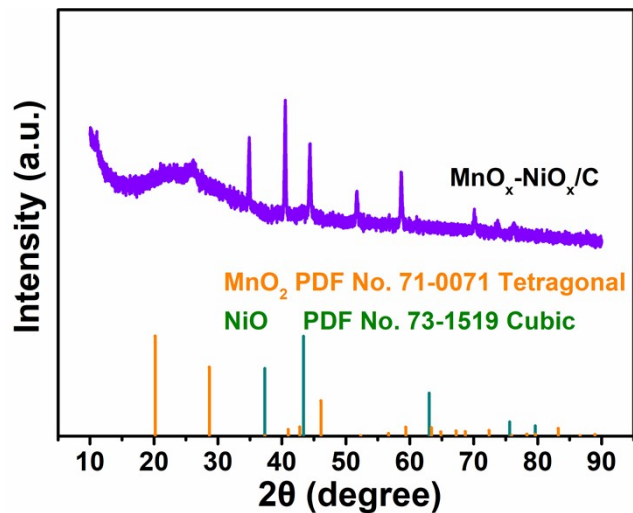


Figure S1 XRD pattern of MnO_x-NiO_x/C.

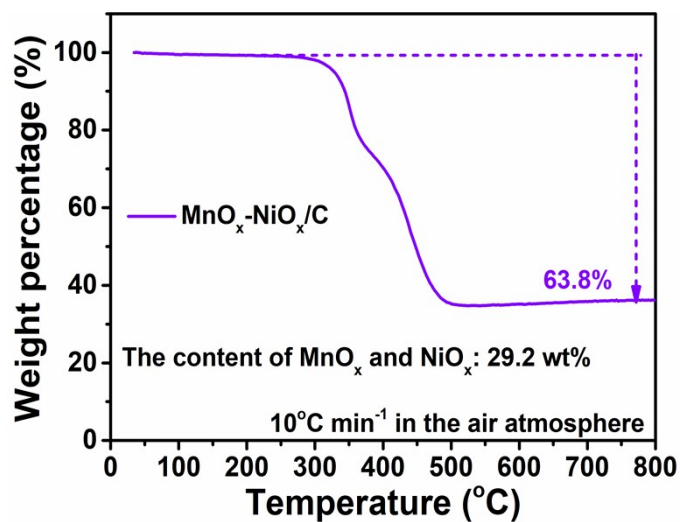


Figure S2 TGA curve of MnO_x-NiO_x/C.

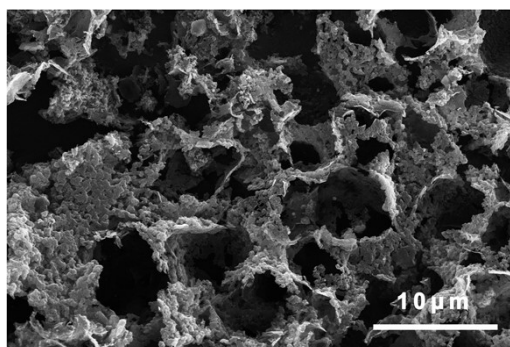


Figure S3 SEM image of MnO_x-NiO_x/C.

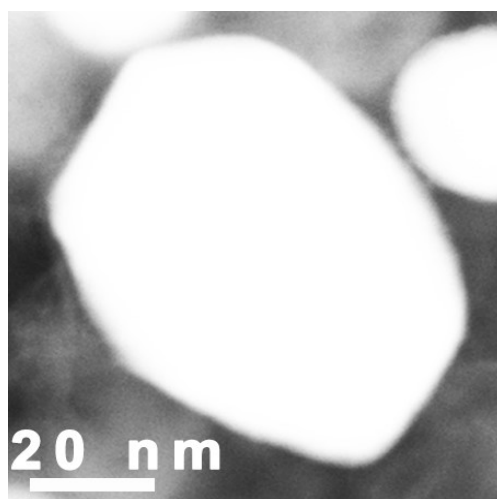


Figure S4 Bright field TEM image of $\text{MnO}_x\text{-NiO}_x/\text{C}$.

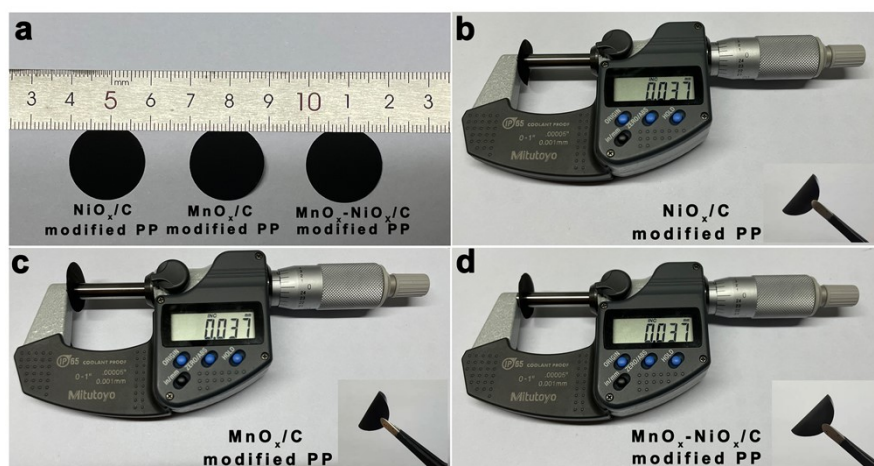


Figure S5. (a) The optical photographs of NiO_x/C modified PP separator, MnO_x/C modified PP separator and $\text{MnO}_x\text{-NiO}_x/\text{C}$ modified PP separator. The thickness testing and flexibility show (as the insert) of (b) NiO_x/C modified PP separator, (c) MnO_x/C modified PP separator and (d) $\text{MnO}_x\text{-NiO}_x/\text{C}$ modified PP separator.

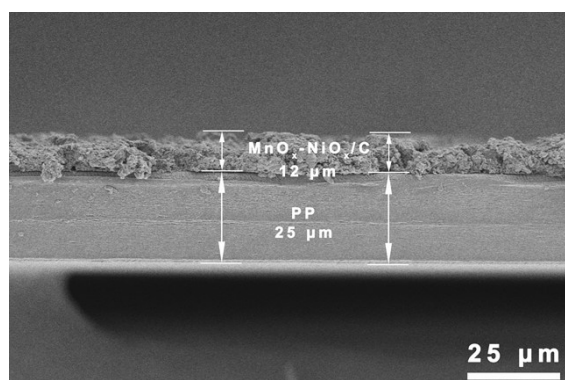


Figure S6 The cross-sectional SEM image of PP separator modified by $\text{MnO}_x\text{-NiO}_x/\text{C}$.

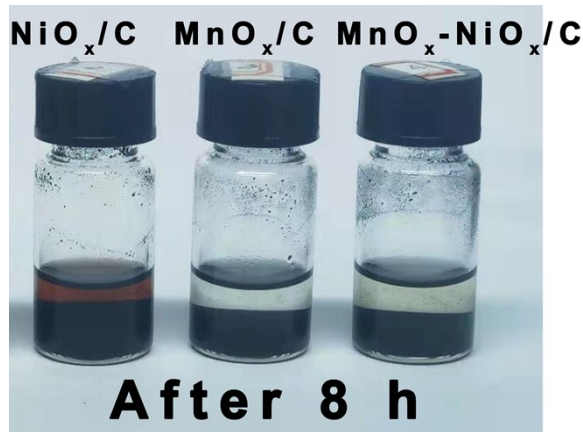


Figure S7 The photograph of color comparison of Li_2S_8 solution after adding NiO_x/C , MnO_x/C and $\text{MnO}_x\text{-NiO}_x/\text{C}$ for 8 h.

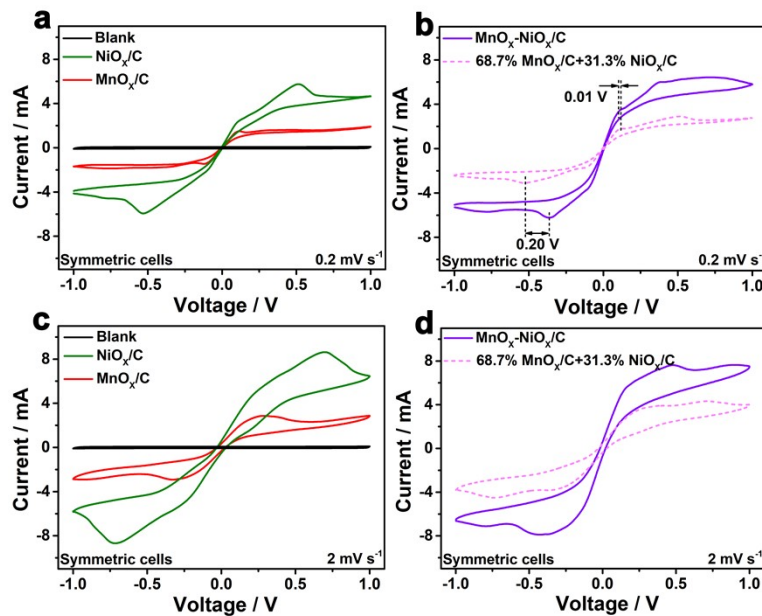


Figure S8. (a) CV curves of the symmetric cells with NiO_x/C electrodes and MnO_x/C electrodes using Li_2S_8 electrolyte or Li_2S_8 -free electrolyte at a scan rate of 0.2 mV s^{-1} . (b) CV curves of the symmetric cells with $\text{MnO}_x\text{-NiO}_x/\text{C}$ electrodes using Li_2S_8 electrolyte or Li_2S_8 -free electrolyte at a scan rate of 0.2 mV s^{-1} and the CV curve obtained by calculation and simulation according to the CV curve in Figure S8a and the ICP results in Table S1. (c) CV curves of the symmetric cells with NiO_x/C electrodes and MnO_x/C electrodes using Li_2S_8 electrolyte or Li_2S_8 -free electrolyte at a scan rate of 2 mV s^{-1} . (d) CV curves of the symmetric cells with $\text{MnO}_x\text{-NiO}_x/\text{C}$ electrodes using Li_2S_8 electrolyte or Li_2S_8 -free electrolyte at a scan rate of 2.0 mV s^{-1} and the CV curve obtained by calculation and simulation according to the CV curve in Figure S8c and the ICP results in Table S1.

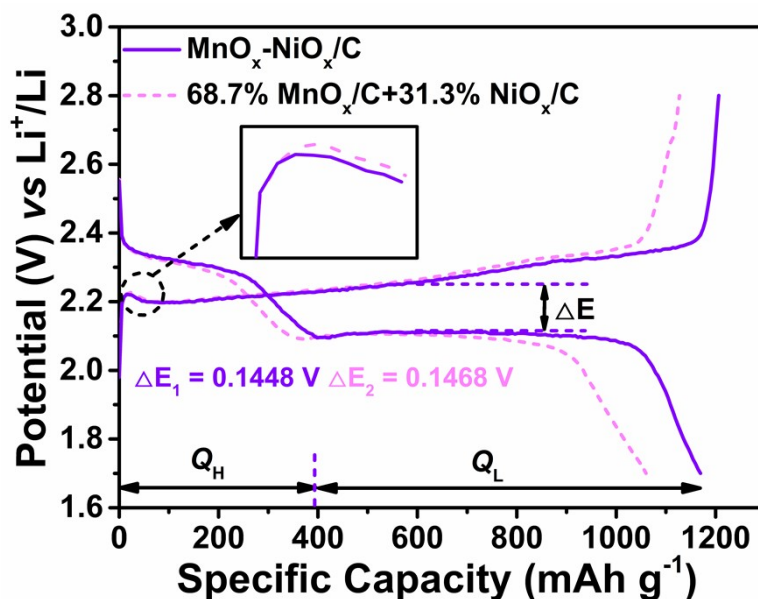


Figure S9 Galvanostatic charge-discharge profile of the cell with $\text{MnO}_x\text{-NiO}_x/\text{C}$ modified PP separator at 0.39 mA cm^{-2} at $E/S = 23 \text{ } \mu\text{L mg}^{-1}$, comparing to a calculated result (dotted line in pink) based on galvanostatic charge-discharge profiles of NiO_x/C modified PP cell and MnO_x/C modified PP cell.

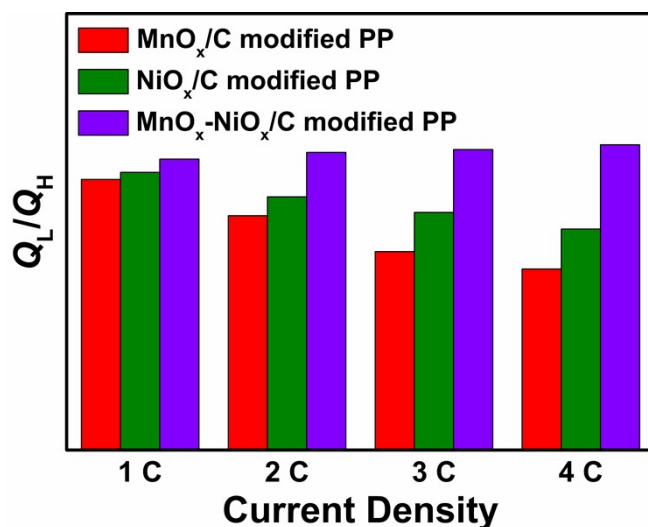


Figure S10 The Q_L/Q_H ratio at different current densities of cells with NiO_x/C , MnO_x/C and $\text{MnO}_x\text{-NiO}_x/\text{C}$ modified PP separators at $E/S = 23 \text{ } \mu\text{L mg}^{-1}$.

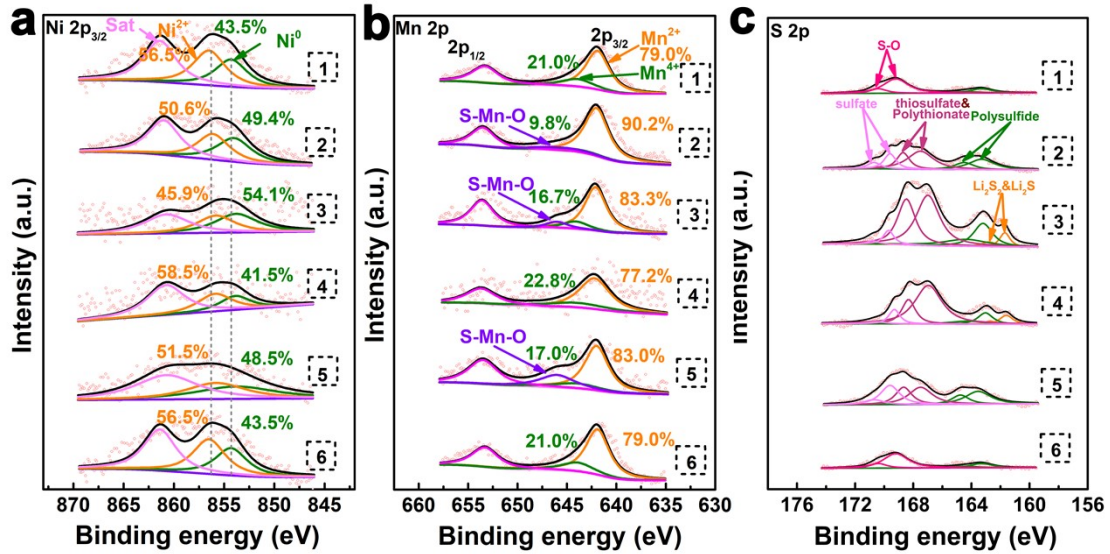


Figure S11. XPS spectras of (a) Ni 2p, (b) Mn 2p and (c) S 2p of MnO_x-NiO_x/C modified PP separator of cells during different discharging/charging stages.

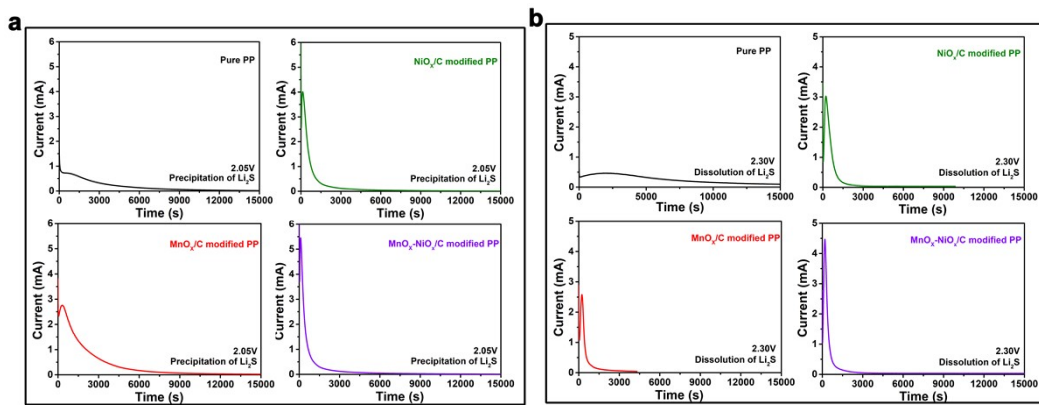


Figure S12. (a) Potentiostatic discharge profile at 2.05 V of cells with Pure PP, NiO_x/C, MnO_x/C and MnO_x-NiO_x/C modified PP separators for evaluating precipitation kinetics of Li₂S with Li₂S₈ catholyte. (b) Potentiostatic charge profiles at 2.30 V of cells with Pure PP, NiO_x/C, MnO_x/C and MnO_x-NiO_x/C modified PP separators for evaluating dissolution kinetics of Li₂S with Li₂S₈ catholyte.

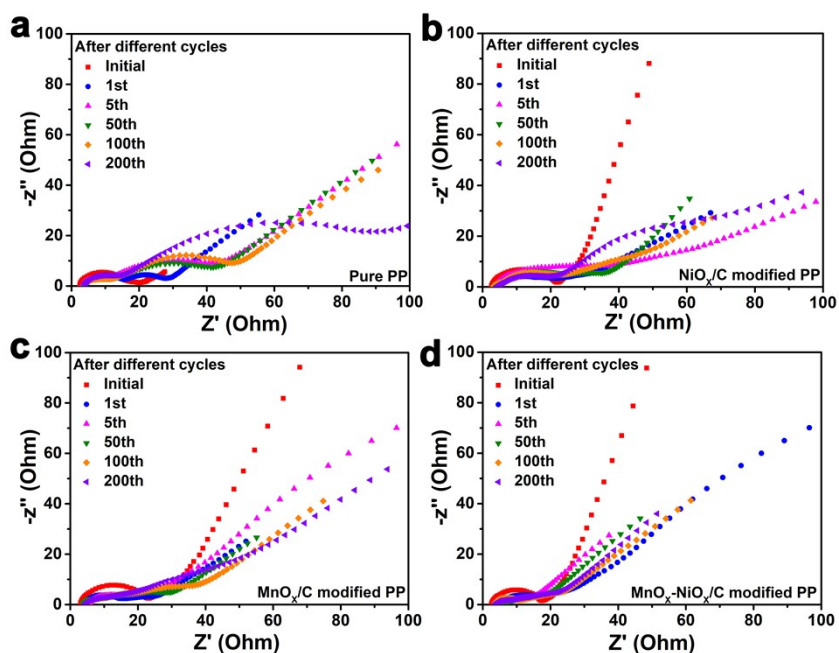


Figure S13. Electrochemical impedance spectra (EIS) of cells with (a) Pure PP, (b) NiO_x/C , (c) MnO_x/C , and (d) $\text{MnO}_x\text{-NiO}_x/\text{C}$ modified PP separators after different cycles (1 C).

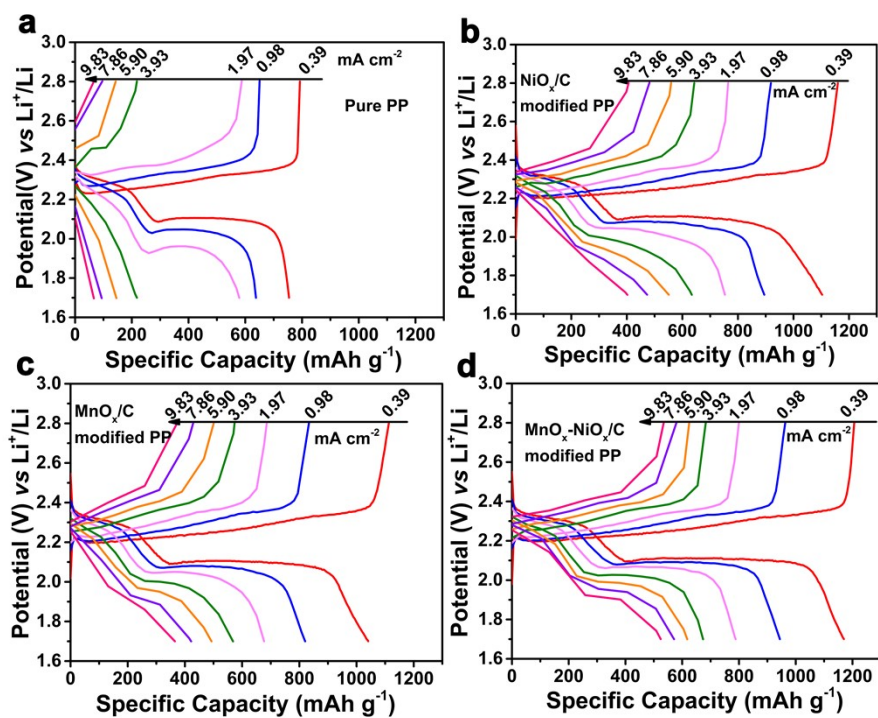


Figure S14. Galvanostatic charge-discharge profiles of cells with separator of (a) Pure PP, (b) NiO_x/C modified PP, (c) MnO_x/C modified PP and (d) $\text{MnO}_x\text{-NiO}_x/\text{C}$ modified PP at different current densities at $E/S = 23 \mu\text{L mg}^{-1}$.

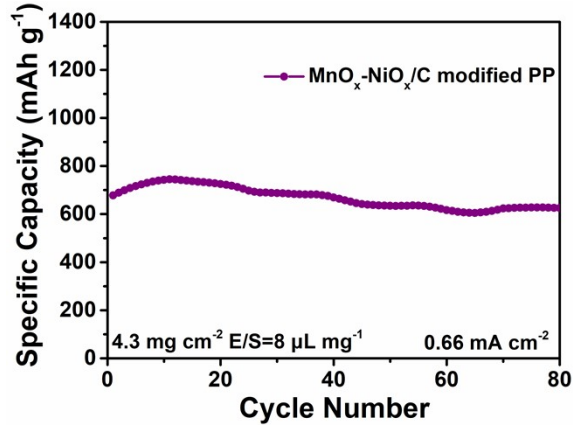


Figure S15. Cycling performance of cell with $\text{MnO}_x\text{-NiO}_x/\text{C}$ modified PP separator at 0.66 mA cm^{-2} with a sulfur loading of 4.3 mg cm^{-2} at $\text{E/S} = 8 \text{ } \mu\text{L mg}^{-1}$.

Table S1 ICP analysis of $\text{MnO}_x\text{-NiO}_x/\text{C}$.

Sample	The mass concentration		Molar ratio of Mn to Ni
	Mn	Ni	
$\text{MnO}_x\text{-NiO}_x/\text{C}$	32.8 mg L^{-1}	15.8 mg L^{-1}	2.2 : 1

Table S2 The fitting EIS results of cells with Pure PP, NiO_x/C , MnO_x/C and $\text{MnO}_x\text{-NiO}_x/\text{C}$ modified PP separators after 200th discharging (1 C).

Modified cells	200 th discharging R_{SEI}/Ω	200 th discharging R_{ct}/Ω
Pure PP	27.6	110.2
NiO_x/C modified PP	21.2	78.1
MnO_x/C modified PP	23.2	95.6
$\text{MnO}_x\text{-NiO}_x/\text{C}$ modified PP	12.6	39.8